

# Uncertainty Quantification in the Directed Energy Deposition Process Using Deep Learning-Based Probabilistic Approach

T.Q.D. Pham<sup>1,3,a</sup>, T.V. Hoang<sup>2,b</sup>, X.V. Tran<sup>1,c\*</sup>, S. Fetni<sup>3,d</sup>, L. Duchêne<sup>3,e</sup>,  
H.S. Tran<sup>3,f</sup>, and A.M. Habraken<sup>3,4,g</sup>

<sup>1</sup>Institute of Strategy Development, Thu Dau Mot University, 75100 Binh Duong Province, Vietnam

<sup>2</sup>Chair of Mathematics for Uncertainty Quantification, RWTH-Aachen University, 52056 Aachen, Germany

<sup>3</sup>University of Liège, MSM Unit, Allée de la Découverte, 9 B52/3, B 4000 Liège, Belgium

<sup>4</sup>Fonds de la Recherche Scientifique de Belgique (F.R.S-FNRS)

<sup>a</sup>pqducthinhbka@gmail.com, <sup>b</sup>hoang.tr.vinh@gmail.com, <sup>c</sup>xuantv@tdmu.edu.vn,

<sup>d</sup>S.Fetni@uliege.be, <sup>e</sup>L.Duchene@ulg.ac.be, <sup>f</sup>hstran@uliege.be, <sup>g</sup>anne.habraken@uliege.be

**Keywords:** Uncertainty quantification, deep learning, directed energy deposition process, melting pool

**Abstract.** This study quantifies the effects of uncertainty raised from process parameters, material properties, and boundary conditions in the directed energy deposition (DED) process of M4 High-Speed Steel using deep learning (DL)-based probabilistic approach. A DL-based surrogate model is first constructed using the data obtained from a finite element (FE) model, which was validated against experiment. Then, sources of uncertainty are characterized by the probabilistic method and are propagated by the Monte-Carlo (MC) method. Lastly, the sensitivity analysis (SA) using the variance-based method is performed to identify the parameters inducing the most uncertainty to the melting pool depth. Using the DL-based surrogate model instead of solely FE model significantly reduces the computational time in the MC simulation. The results indicate that all sources of uncertainty contribute to a substantial variation on the final printed product quality. Moreover, we find that the laser power, the convection, the scanning speed, and the thermal conductivity contribute the most uncertainties on the melting pool depth based on the SA results. These findings can be used as insights for the process parameter optimization of the DED process.

## Introduction

Additive Manufacturing (AM) is a versatile technology to build complex three-dimensional objects by successively adding material layer by layer. Directed Energy Deposition (DED) is an AM technique adapted to repair operations. Currently, DED is widely used to fabricate metal components in many applications such as aerospace [1], bio-design [2].

Some of the barriers limiting the wide adaption of DED in many industrial sectors are their high upfront investment costs and the lack of consistent quality of the printed parts. In addition, during the DED process, various sources of uncertainty can affect the temperature evolution, which is an important parameter to determine the final microstructure [3] of the printed piece. Sources of uncertainty include properties of the input materials, process parameters, and environmental conditions [3, 4, 5].

A key to better analyze and resolve the above problem is using uncertainty quantification (UQ) during the DED process. However, a very large number of input-output pairs will be required in the propagation and optimization steps [5]. Therefore, using experiments and/or finite element (FE) simulation is impractical. Hence, Deep Learning (DL) is a promising tool to build a surrogate model to replace the role of the FE model [6].

The efforts of performing UQ in AM field are mainly observed at the laser powder bed fusion (L-PBF) process [7,8], and thus limits its generalization to other AM processes such as DED. Based on these backgrounds, we develop a DL-based probabilistic approach for the uncertainty

quantification in the DED process to investigate the influence of input uncertain parameters on the quality of the final printed products.

This paper is organized as follows: Firstly, the methodology including characterization and propagation of uncertainties are first introduced. Secondly, the verification of deep learning-based surrogate model is discussed. Thirdly, the propagation of uncertainty to obtain uncertain characteristics of the temperature field and melting pool size are performed. Finally, the sensitivity analysis result is presented.

## Methodology

This study focuses on bulk experiments of the M4 High-Speed Steel manufactured by the DED process. The probabilistic method uses mathematical techniques to characterize the DED process uncertainty sources as one or more random variables. The input uncertainty is then propagated to the output using a computational model. The temperature field can be expressed as

$$T = f(\mathbf{q}, \mathbf{X}), \quad (1)$$

where

$$\mathbf{q} = [x, y, z, t, \mu_1, \dots, \mu_M, \vartheta_1, \dots, \vartheta_P] \quad (2)$$

is a multi-dimensional vector of spatial coordinates  $(x, y, z)$ , time  $(t)$ , material properties  $\mu_1, \dots, \mu_M$  of the powder and process parameters  $\vartheta_1, \dots, \vartheta_P$  of the AM process and  $f$  is the computational model. The probabilistic method is then used to model each uncertainty parameter  $\mathbf{X}$  in  $\mathbf{q}$  as the probability distribution and rely on the probability theory to determine their impact on the temperature field and melting pool depth. Hereafter, we present the essential ingredients of the probabilistic method as characterization of uncertainty and propagation of uncertainty.

### Characterization of uncertainty

The probabilistic method begins with characterizing the uncertain parameters as a random variable  $\mathbf{X} = (X_1, X_2, \dots, X_n)$  with the values in  $\mathbb{R}^n$  and represent them as a probability distribution function (PDF) as

$$\pi_{\mathbf{X}} = \pi_{(X_1, X_2, \dots, X_n)}. \quad (3)$$

In this study, we consider the uncertainties from process parameters, material properties, and boundary conditions.

For (i), we consider four process parameters: laser power, scanning speed, ambient temperature, and substrate preheating temperature, as observed in several studies [4,5].

For (ii), we consider the thermal conductivity and heat capacity as the uncertain parameters because the precise values of these properties at high temperatures are unknown [3]; computational models may have uncertainty due to these unknown macroscopic values.

For (iii), we consider the convection and radiation of the clad as input uncertain parameters. Indeed, accurate measurement of these parameters is a challenge and is critical in modeling the AM processes [2,3].

We adopt a probabilistic framework to quantify the impact of uncertainties on the temperature field and melting pool depth. We model the input uncertain parameters followed by the uniform distribution. Their bounded range are listed in Table 1.

Table 1. Eight uncertain parameters and their bounded range

Input uncertain parameter		Notation	Bounded range
Process parameters	Effective laser power	$\mathcal{P}$	[0.97, 1.03]
	Scanning speed	$v$	[335, 365]
	Ambient temperature	$T_a$	[284.15, 312.15]
	Substrate preheating temperature	$T_s$	[555.15, 591.15]
Boundary conditions	Convection	$h$	[200, 300]
	Radiation	$\varepsilon$	[0.8, 1]
Material properties	Thermal conductivity	$\alpha_k$	[0.93, 1.07]
	Heat capacity	$\alpha_c$	[0.95, 1.05]

### Propagation of uncertainty

Once the input uncertain parameters are characterized, they will be propagated using the Monte-Carlo (MC) method accelerated by the DL-based surrogate model to obtain the distribution of temperature field and melting pool depth. Hereafter, we discuss the ML method and the DL-based surrogate model.

#### Monte-Carlo method

In this study, the MC method is chosen based on its simplicity. The MC method generates  $n$  independent and identically distributed (i.i.d.) samples from the PDF  $\pi_{\mathbf{X}}$ , and use the computational model  $f$  to obtain the temperature distribution. After getting these i.i.d. samples, the mean  $m_T$  and the variance  $\sigma_T^2$  can be approximated as:

$$m_T \approx \frac{1}{n} \sum_{i=1}^n T_i, \quad \sigma_T^2 \approx \frac{1}{n} \sum_{i=1}^n (T_i - m_T)^2. \quad (4)$$

The approximation accuracy in Eq. (4) depends on the square root of the number of samples  $n$  [4]. Consequently, the MC method requires a very large number of simulations  $f$  to ensure a good approximation. However, the computational cost of the FE model remains expensive. Therefore, a DL-based surrogate model is often constructed to gain computational efficiency.

#### DL-based surrogate model

This section describes the DL-based surrogate model to approximate the relationship between the uncertain input variables and the quantity of interests (QoIs). The feedforward neural network (FFNN) model is chosen in this study, owing to its advantages in approximating complex functions over high dimensional spaces. The FFNN-based surrogate model has been developed in our previous study [6], which is applied for the only variation of  $Q_{\text{laser}}$ . In this study, we extend this model to account for the variation of eight input uncertain parameters as listed in Table 1.

The FFNN-based surrogate model can be considered as a function  $g$  such that

$$g(\mathbf{q}, \mathbf{X} | \mathbf{W}) \approx f(\mathbf{q}, \mathbf{X}), \quad (5)$$

where  $\mathbf{W}$  denotes the weights and biases of the model. The FFNN-based surrogate model is trained on the training dataset  $\mathbf{D}_T$  consisted of different FE simulations as 5, 10, 15, 18, 21, 25, and 28, with different values of DED uncertain parameters ( $X_1, X_2, \dots, X_8$ ).

Once the surrogate model is built and validated against the computational model, the MC method maps the uncertain input variable distribution through this FFNN-based model to obtain the temperature field distribution. Consequently, the statistical descriptions of the temperature  $T$  can be approximated as

$$m_T \approx m_T^g = \frac{1}{n} \sum_{i=1}^n \hat{T}^{(i)}, \quad \sigma_T^2 \approx (\sigma_T^g)^2 = \frac{1}{n} \sum_{i=1}^n (\hat{T}^{(i)} - m_T^g)^2, \quad (6)$$

where the subscript  $g$  serves to distinguish the surrogate model from the FE numerical simulation. To assess the global and local performance of the FFNN-based model, we use the  $R^2$  metric and relative error  $\alpha$ , respectively defined as

$$R^2 = 1 - \frac{\sum_{j=1}^{N_V} (g(\mathbf{q}^{(j)}, \mathbf{X}^{(j)}) - T^{(j)})^2}{\sum_{j=1}^{N_V} (\bar{T} - T^{(j)})^2}, \quad (\{\mathbf{q}^{(j)}, \mathbf{X}^{(j)}\}, T^{(j)}) \in \mathbf{D}_V, \quad (7)$$

where  $N_V$  is the size of the validation set  $\mathbf{D}_V$  and  $\bar{T}$  is the mean temperature.

### Sensitivity analysis using variance-based method

This section presents the sensitivity analysis (SA) using the variance-based method. Performing the SA can help characterize which uncertain parameters contribute the most to the uncertainty of the quantity of interests. This study performs the SA using the variance-based method [4, 5] owing to its straightforward interpretation. We perform the SA only on the melting pool depth for demonstrating the framework.

## Results and Discussion

This section presents the verification of the FFNN-based surrogate model, the results obtained from the uncertainty propagation, the computational efficiency assessment, and the SA to identify the most impact input uncertain parameter to the melting pool depth.

### Verification of the FFNN-based surrogate model

In order to choose a least number of FE simulations in the training data while still maintaining a good accuracy, we train seven independent FFNN models with different FE simulations as 5, 10, 15, 18, 21, 25, and 28. Fig. 1 shows the range and mean of  $R^2$  values evaluated within data obtained the testing dataset  $\mathbf{D}_\tau$  of these seven models. As shown in Fig. 1, the mean  $R^2$  value converges with the  $n_{FE} \geq 21$ . Consequently, we choose  $n_{FE} = 21$  to construct the FFNN-based surrogate model to predict the temperature evolutions with acceptable accuracy.

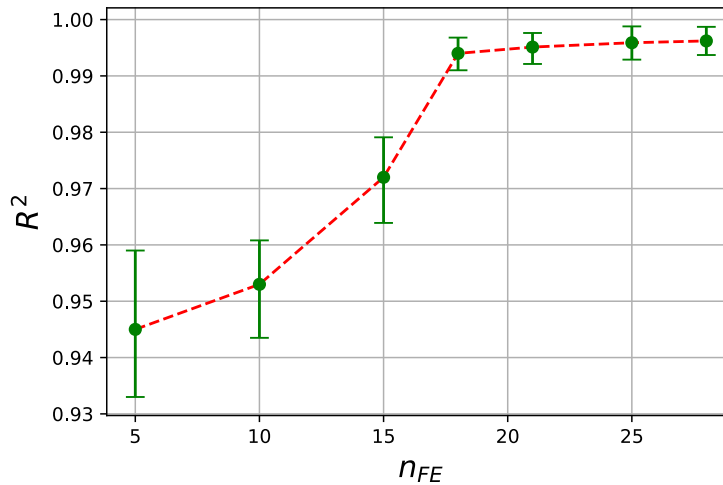


Fig. 1. The range and mean of  $R^2$  values evaluated within the testing dataset  $\mathbf{D}_\tau$

### Propagation of uncertainties

This section presents the results obtained by the uncertainty propagation step. First, we check the convergence analysis of MC simulation. Then, we show the obtained uncertainty characteristics of the temperature field and melting pool depth. Finally, we assess the computational efficiency of the FFNN model.

#### Convergence analysis of MC simulation

Fig. 2 shows the standard deviation of the maximum melting pool depth (i.e., the one in last layer) with respect to the number of MC simulations ( $n_{MC}$ ). As observed in Fig. 2, the standard deviation does not change much after  $n_{MC} = 1000$ , and thus, we choose 1000 as the number of MC simulations to perform the uncertainty propagation.

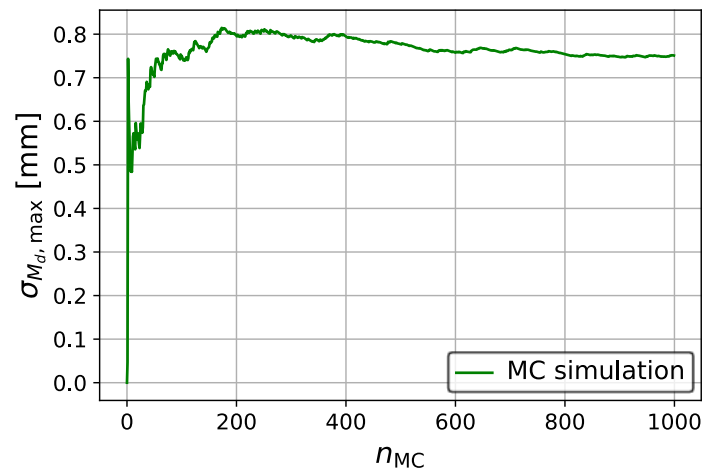


Fig. 2. The standard deviation of the maximum melting pool depth with respect to the number of MC simulations

#### Uncertainty characteristics of the temperature field

This section shows the obtained uncertainty characteristics of the temperature field assessed at two clad points, as  $P_1$  (located at the middle of the first printed layer) and  $P_2$  (located at the middle of the 9<sup>th</sup> printed layer).

Figs. 3(a) and 3(b) show 1000 MC samples of the temperature evolutions at the two selected points, including points  $P_1$  and  $P_2$ . As shown in Fig 3, the considered uncertainties presented in Sec. 2.2 contribute to a potent variation of the temperature evolutions. In particular, the variation ups to 9.4% compared with their mean values. Moreover, the temperature standard deviation increases with the layer number, which is due to the uncertainty accumulation.

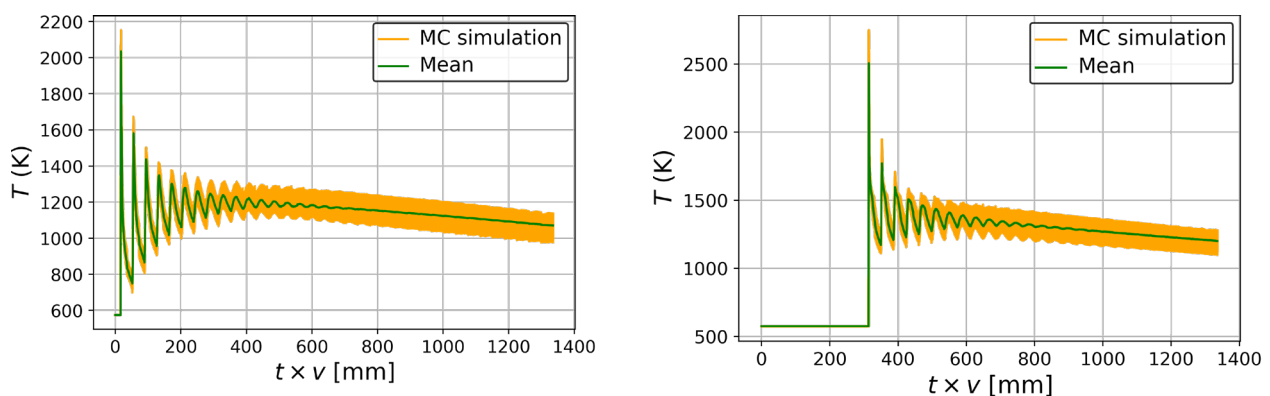


Fig. 3. 1000 MC samples of the temperature evolutions of point  $P_1$  and  $P_2$ . The horizontal axis expresses the cumulative distance of the laser assuming one track per layer

### Uncertainty characteristics of the melting pool depth

This section shows the obtained uncertainty characteristics of the melting pool depth ( $M_d$ ). Fig. 4 shows the empirical distribution of the melting pool depth with 1000 MC simulations. The results show that the melting pool depth range increases significantly when increasing the layer number. As a consequence, in the DED process, it is challenge to obtain a steady melting pool depth [3].

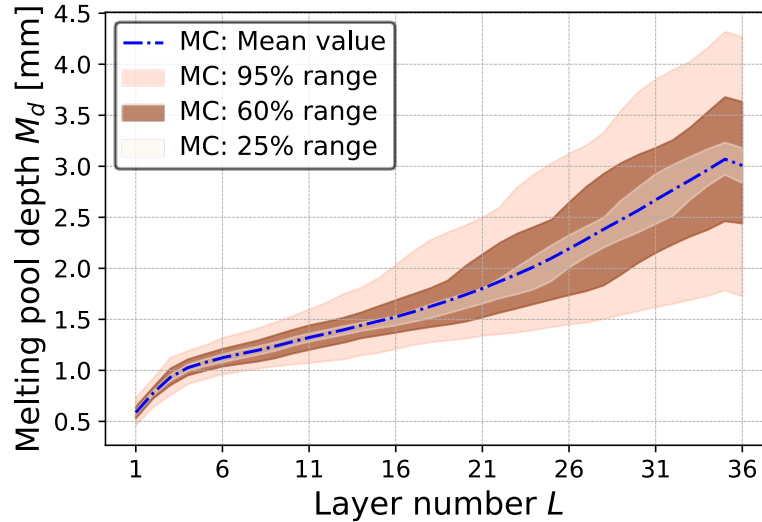


Fig. 4. Empirical distribution of the melting pool depth with 1000 MC simulations

### Computational efficiency assessment

Table 2 compares the computational cost needed to perform a direct MC simulation, which uses the FE and FFNN-based surrogate models. For one MC simulation, the FFNN-based surrogate model only takes 12 s to compute the statistical description of the temperature field, which reduces 181 compared with the FE model. As a consequence, 3.3 hours are required for 1000 MC simulations with the surrogate model, whereas the FE model requires 600 hours (25 days). In summary, using the FFNN-based surrogate model instead of the FE model reduces the computational cost significantly in the MC simulation.

Table 2. Computational costs needed to perform a direct MC simulation, which uses the FE and FFNN-based surrogate model

Number of MC simulation	FE model (h)	FFNN-based surrogate model (h)
1	0.6	0.0033 (12 s)
1000	600	3.3

In brief, the proposed framework allows quantifying the variation of the temperature field and melting pool depth with the uncertainty raised from the process parameters, material properties, and boundary conditions.

### Sensitivity analysis

This section presents the results obtained by the sensitivity analysis. Fig. 5 shows the Sobol indices for the melting pool depth in the final layer of the product. As observed in Fig. 5, convection, laser power, scanning speed, and thermal conductivity induce the most uncertainties to the final product quality. A focus on these properties should be presented while optimizing the manufacturing process because it determines the microstructure genesis, which is responsible for part properties.

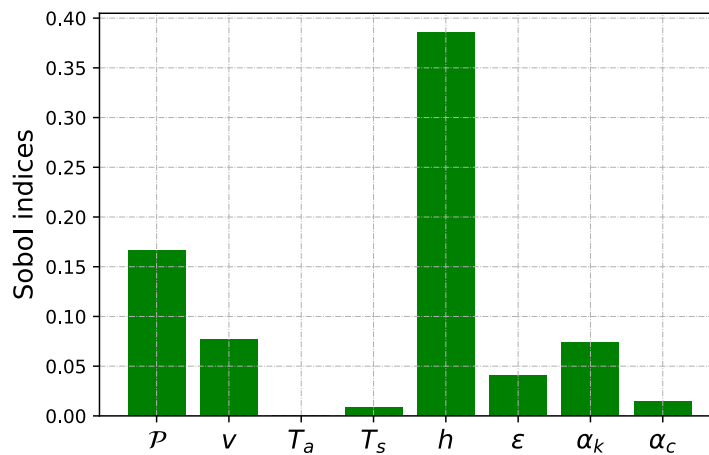


Fig. 5. The Sobol indices for each input uncertain parameter in inducing the uncertainties in the melting pool depth

### Summary

In this paper, the effects of uncertainty in process parameters, material properties, and boundary conditions on the directed energy deposition (DED) process of M4 High-Speed Steel are quantified using deep learning (DL)-based probabilistic approach. A DL-based surrogate model is first constructed using the data obtained from a finite element (FE) model, which was validated against the experiment. The DL-based surrogate model reduces the computational cost significantly while assuring the accuracy of 99% compared with the FE model. Then, the uncertainty characteristic of the temperature field and melting pool depth is quantified with the uncertainty from process parameters, material properties, and boundary conditions. The results indicate that all sources of uncertainty lead to a potent variation of the temperature field and melting pool depth. Moreover, the sensitivity analysis results show that the convection, laser power, scanning speed, and thermal conductive induce the most uncertainty to the melting pool depth. These findings would provide valuable insights for the process parameter optimization of the DED process to improve the quality of the printed parts. The process optimization under uncertainty to get the steady melting pool will be performed for future works.

### Acknowledgement

This work was funded by Vingroup and supported by Vingroup Innovation Foundation (VINIF) under project code **VINIF.2020.DA15**.

### References

- [1] Uriondo, A., Esperon-Miguez, M., & Perinpanayagam, S.. The present and future of additive manufacturing in the aerospace sector: A review of important aspects. *Proceedings of the Institution of Mechanical Engineers, Part G: Journal of Aerospace Engineering*, 229, (2015), 2132-2147.
- [2] Culmone, C., Smit, G., & Breedveld, P. (2019). Additive manufacturing of medical instruments: A state-of-the-art review. *Additive Manufacturing*, 27 (2019)., 461-473.
- [3] Jardin, R. T., Tchuindjang, J. T., Duchêne, L., Tran, H. S., Hashemi, N., Carrus, R., Mertens, A., & Habraken, A. M. Thermal histories and microstructures in Direct Energy Deposition of a High Speed Steel thick deposit. *Materials Letters*, 236, (2019). 42-45.

- [4] Hu, Z., & Mahadevan, S., Uncertainty quantification and management in additive manufacturing: current status, needs, and opportunities. *The International Journal of Advanced Manufacturing Technology*, 93, (2017), 2855-2874.
- [5] Hu, Z., & Mahadevan, S. (2017). Uncertainty quantification in prediction of material properties during additive manufacturing. *Scripta materialia*, 135, 135-140.
- [6] T.Q.D. Pham, T.-V. Hoang, X.V. Tran, Q.T. Pham, S. Fetni, L. Duchêne, H.S. Tran, A.-M. Habraken. Fast and accurate prediction of temperature evolutions in additive manufacturing process using deep learning, *Journal of Intelligent Manufacturing*, (2021), in press.
- [7] Tapia, G., King, W., Johnson, L., Arroyave, R., Karaman, I., & Elwany, A. (2018). Uncertainty propagation analysis of computational models in laser powder bed fusion additive manufacturing using polynomial chaos expansions. *Journal of Manufacturing Science and Engineering*, 140(12).
- [8] Lopez, F., Witherell, P., & Lane, B. (2016). Identifying uncertainty in laser powder bed fusion additive manufacturing models. *Journal of Mechanical Design*, 138(11).